A steady-state numerical approach for the thermo-structural analysis of a cryogenic piston pump

Stefano Cioni[1*], Francesco Balduzzi[1], Luca Romani[1], Luca Sambri[2], Luca Marianetti[2] and Giovanni Ferrara[1]

[1] Department of Industrial Engineering (DIEF), Università degli Studi di Firenze, Firenze, Italy
[2] 3P Prinz s.r.l., Coselli, Italy

*E-mail: stefano.cioni@unifi.it

Abstract. The process of liquefaction of gaseous fuels, such as natural gas or hydrogen, is an essential technology that helps reduce transportation costs over long distances. Cryogenic piston pumps play a critical role in these systems, as they compress the fuel up to 700 bar before vaporization and storage in high-pressure vessels. Due to the extreme temperatures and pressures involved, the design of these machines poses a significant challenge from the thermal and structural point of view. This work presents the application of a simplified numerical approach for evaluating the thermally induced stresses and deformations through a de-coupled thermo-structural three-dimensional analysis of a prototype cryogenic piston pump. Thermal simulations of the solid domain are carried out to assess the steady-state temperature distribution of the pump. The heat transfer between the pump and cryogenic liquid is computed using three-dimensional steady-state CFD simulations of the suction and discharge phases. Heat generated by friction during the working cycle of the pump and external natural convection are calculated and imposed as a heat source in the simulations. The steady-state temperature distribution is imposed in a finite-element steady-state three-dimensional structural simulation to evaluate the combined effect of thermal loads induced by the cryogenic temperatures and loads induced by the high working pressures. Results show how the proposed methodology can assist in the design of cryogenic piston pumps by offering valuable insights into the most critical aspects of these machines.

1. Introduction

One of the crucial issues hampering the spread of gaseous fuels such as methane or hydrogen, is their limited volumetric density. This impacts not only possible applications but also transportation costs from the production site to the end user. Over long distances, the best economic performance is achieved by liquefying the gas, which is then transported on modified ships. Finally, the fuel is either gasified and stored in high pressure vessels or provided to the end user as a cryogenic liquid.

In these systems, cryogenic piston pumps are used to mobilize and pressurize the cryogenic liquid up to 700 bar, depending on the application.

The design of reciprocating cryogenic piston pumps has to tackle multiple issues. First, boil-off of the cryogenic liquid must be minimized as this leads to a reduction of the efficiency or even shut down of the pump in the most severe cases. Evaporation may occur both due to cavitation, when the internal pressure losses of the pump cause the pressure to fall below the saturation value, or due to heat transfer with the pump body.

Additionally, the design of these machines needs to account for the combination of structural and thermal loads, induced by the high working pressures (up to 700 bar) and cryogenic

temperatures. Therefore, adequate materials have to be chosen to provide adequate reliability and characteristics in these conditions.

Despite these multiple challenges, the design of cryogenic piston pumps is still based on standard design approaches, based on the knowledge acquired by the industry over the years. Indeed, only a limited amount of works have been published concerning the design of these machines, which have focused on experimental testing of prototypes or existing machines.

Li et al.[1] tested a submerged liquid hydrogen cryogenic piston pump applied to a refueling station. The pump was capable of reliable operation for a period of 6 months. Biermann and Kohl [2] tested a five-cylinder variable-displacement cryogenic piston pump at different rotational speed, defining the cavitation performance of the pump. The effect of rotational speed on the volumetric efficiency of a liquid helium cryogenic piston pump was evaluated by Lue et al. [3]. Results showed how at lower rotational speeds the efficiency is reduced due to liquid evaporation. The effect of piston geometry on the leakage flow was investigated by Yamane et al.[4]. Multiple configurations were tested experimentally, and the optimal solution was identified.

To the best of the author's knowledge, however, no works have been published concerning the application of simulation methods to cryogenic piston pumps.

Nevertheless, these methods can provide further insight into the physical phenomena governing the pump working cycle and aid the design process. Previous work by the authors [5] has shown how three-dimensional steady-state CFD simulations can aid the design process of a prototype cryogenic piston pump in order to reduce internal pressure losses and improve the working range by limiting the risk of cavitation.

In this work, a steady-state simplified simulation approach is described, that combines CFD, thermal, and structural simulations to provide insight into the steady state response of a prototype cryogenic piston pump. The objective is to evaluate the steady-state thermal response of the prototype, to verify that friction and ambient heat transfer do not lead to excessive temperatures. The results are combined with structural simulations to verify the structural integrity of crucial components and the coupling between the piston and the cylinder against design tolerances.

This work is structured as follows: the prototype piston pump is described in Section 2. In Section 3 the methodology used is presented, followed by a summary of the main results in Section 4. Finally, conclusions and possible future work are described in Section 5.

2. Pump Geometry

In this work a reciprocating single-piston cryogenic pump is analyzed (Figure 1). The pump is designed to reach a maximum pressure of 350 bar. The pump is designed to be connected to a cryogenic vessel through a suction and return line in a thermosyphon configuration. The suction circuit was analyzed in previous work by the authors [5] to identify possible improvements to limit cavitation of the fluid. In this prototype, the liquid enters an internal volume surrounding the body of the pump, which cools down the machine during its operation and maintains the working temperature even after shut-down. Insulation from the external ambience is achieved through a cylindrical vacuum chamber enclosing the lateral surface of the pump.

From the inner volume, the liquid enters the cylinder during the suction phase through a series of channels co-axial with the piston. The suction valve is automatic and opens due to the pressure difference across the valve. After the suction phase, the piston moves towards the top dead center and the suction valve closes. When the pressure within the cylinder surpasses the pressure value in the discharge vessel the automatic discharge valve opens, and the cryogenic

liquid is pushed into the discharge line. The discharge duct is a single channel situated at the top of the cylinder.

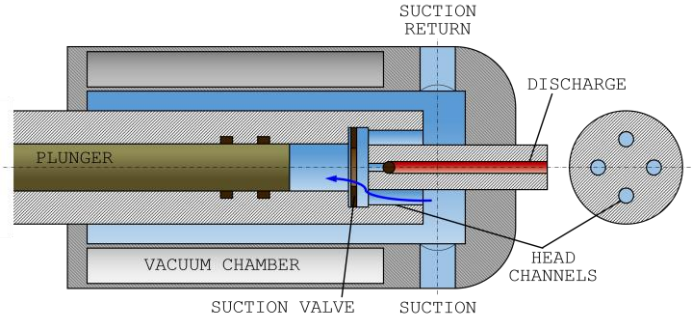

Figure 1. Simplified scheme of prototype piston pump

In this prototype, the leakage between the piston and cylinder gap is prevented through two fixed ring seals, installed in purpose-built seats on the cylinder surface. The design of the piston seals represents a complex issue as they must reduce both flow leakage and friction between the piston and cylinder surface. In this work, it is assumed that bronze-filled Teflon rings are used, as they guarantee both limited friction and adequate conductivity.

3. Methodology

In this study, a simplified steady-state methodology is presented, as summarized in Figure 2. Fluid dynamic CFD simulations are combined with thermal and structural simulations to provide further insight into the thermal and structural response of the pump.

The thermal simulations are performed to obtain the steady-state temperature distribution of the pump. One of the crucial issues concerns the definition of the boundary conditions. In this work, the heat transfer with the cryogenic liquid is considered by calculating the distribution of the heat transfer coefficient through de-coupled steady-state CFD simulations (see Section 3.1). Additionally, the heat generated by friction and the heat transfer with the external ambient are estimated (see Sect. 3.2).

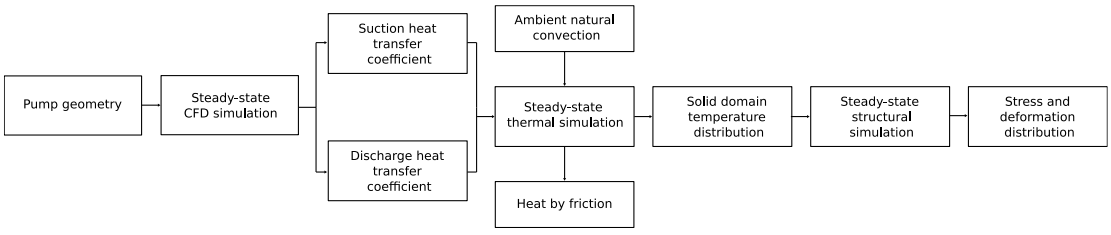

Figure 2. Summary of methodology.

The temperature distribution is then used as an input to the structural simulations (see Sect. 3.3), to evaluate stresses and deformations of critical components under the combined influence of the fluid pressure and thermal stresses induced by temperature gradients.

3.1. CFD simulation setup

The reciprocating pump is characterized by an intrinsically unsteady behaviour, due to the continuous succession of suction and discharge phases. Hence, to perform a coupled simulation of the fluid and solid domain, an unsteady approach is required. In this work, a simplified

methodology is used to evaluate the distribution of the heat transfer coefficient from three-dimensional steady-state CFD simulations.

The suction and discharge phases are analyzed through two different RANS simulations, using an analogous set up to that described by the authors in previous work [5]. Liquid nitrogen is chosen as the working fluid, in order to compare results with possible future experimental campaigns, as the results should be compatible with those obtained using liquid hydrogen [2]. To solve the fluid equations, the liquid domain is discretized into about $15 \cdot 10^6$ elements. The mesh is generated automatically through the commercial software ANSYS Meshing. The core of the fluid domain is discretized using an unstructured tetrahedral mesh. Instead, in the near wall region 24 prismatic elements are used to correctly capture the fluid behaviour. The size of the first element is set to achieve y^+<1 in most of the domain. The RANS simulations are performed using the SST turbulence model to close the fluid equations.

For the suction phase, the total pressure is set at the inlet of the domain and the average piston velocity is imposed at the outlet. For the discharge phase the inlet fluid velocity is set equal to the mean piston velocity and the discharge pressure is imposed at the pump outlet. In both cases the fluid temperature is set equal to the saturation temperature of liquid nitrogen at 5 bar (i.e.77 K) and the wall temperature is set to 87 K. The wall heat flux, Q, is obtained from the simulations, and consequently the heat transfer coefficient is calculated as,

$$HTC = \frac{Q}{T_{wall} - T_f}, \tag{1}$$

where T_{wall} and T_f are the wall and fluid temperature, respectively.

The distribution of the heat transfer coefficient for the suction and discharge phases are averaged. Since in the CFD simulations there is no mass flowrate in the suction circuit during the discharge phase and in the discharge circuit during the suction phase, it is assumed that when the fluid is still during one of the phases, the heat transfer coefficient is reduced by a factor of 10.

In addition to the heat transfer taking place in the suction and discharge lines, the leakage flow between the piston and the seals contributes to the cooling of the cylinder and piston walls. The value of the heat transfer coefficient is calculated using correlations for a flow in a cylindrical gap. In this work, the heat transfer coefficient for the leakage flow was estimated as $1000\ Wm^{-2}K^{-1}$. During the motion of the piston the lateral surface of the cylinder is either exposed to the leakage flow or to the liquid contained within the cylinder. Depending on the distance from the top dead center, the wall of the cylinder is exposed for different time intervals to either the leakage flow or the cylinder flow. For this reason, a linear distribution of the heat transfer coefficient is assumed from the mean cylinder value, for those surfaces that are never covered by the piston, to the leakage value, for the parts of the cylinder that are always facing the piston.

3.2. Thermal simulation setup

In this study, three-dimensional steady-state simulations of the solid domain are performed to estimate the temperature distribution of the pump using the commercial software ANSYS CFX. To solve the heat transfer equations, the solid domain is discretized into about $13 \cdot 10^6$ tetrahedral elements. For each component of the pump the thermal conductivity and density of the material are defined. As the heat transfer in the vacuum chamber is negligible in comparison to the conduction in the metal, the internal surfaces of the vacuum are assumed adiabatic.

In order to solve the heat transfer equation, the boundary conditions must be defined. The heat transfer between the solid and the cryogenic liquid is estimated by imposing a liquid temperature of 77 K and a map of the heat transfer coefficient calculated from the CFD simulations as described in Sect. 3.1.

Additionally, the effect of the heat generated by friction is included in the simulations as a heat source term. The analyzed prototype presents 2 stationary rings in the liner (see Sect. 2), and the friction force is calculated as,

$$F_f = fA(p_1 + p_2) \tag{2}$$

where f is the friction factor, assumed equal to 0.25 between steel and Teflon, A is the total ring area and p_1 and p_2 are the pressures acting on the first and second ring respectively. In this case, it is assumed that the average cycle pressure acts on the first ring and that the suction pressure acts on the second ring.

The power dissipated due to friction is calculated as,

$$P = \frac{F_f V_p}{S_p}, \tag{3}$$

where V_p is the piston velocity, and S_p is the contact surface. The heat generated by friction is split between the piston and the rings proportionally to the thermal conductivity of the materials. In the analyzed prototype, the piston is made from stainless steel and the rings are made from bronze-filled Teflon. Hence, the conductivity of the piston and rings are $\lambda = 10\ WmK^{-1}$ and $\lambda = 0.9\ WmK^{-1}$ respectively. Consequently, it is assumed that 90% of the power dissipated due to friction is transferred to the piston and the remaining 10% is transferred to the Teflon rings.

In the simulations, the heat flux to the piston rings is calculated as,

$$Q = \frac{P}{S} \tag{4}$$

where P is the fraction of total power that is dissipated at the piston rings and S is the contact surface of the rings.

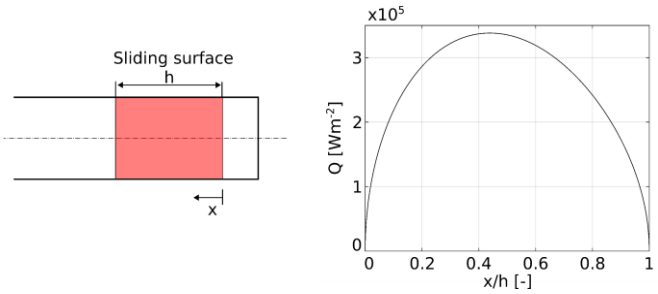

Figure 3. Heat flux distribution along the piston length.

In contrast, the heat flux towards the piston is not homogenous along the contact surface. Indeed, due to the reciprocating motion the heat generated by friction is distributed unevenly along the length of the piston. When the piston is close to the top or bottom dead center the piston speed reaches its lowest value, and the heat generated by friction is reduced. Instead, when the piston is close to the mid-stroke position, it reaches the maximum velocity, and consequently the heat generated by friction reaches its maximum value. Hence, the heat flux can be calculated as a function of the position along the piston using Eq. (3). The resulting heat flux distribution is shown in Figure 3.

Finally, the heat transfer with the external ambient is estimated from available correlations. Given the cylindrical geometry of the pump, a constant heat transfer is assumed and its value is calculated from the correlation of McAdams,

$$Nu = 0.13(GrPr)^{1/3}, \quad (5)$$

Where Nu is the Nusselt number, and Gr and Pr are the Grashof and Prandtl numbers, respectively. The heat transfer coefficient is calculated from the Nusselt number as,

$$HTC = \frac{Nu \cdot k}{L}, \quad (6)$$

where k is the thermal conductivity of air and L is the length of the pump.

3.3. Structural simulation setup

In the second part of this work, simplified structural simulations have been carried out to verify some critical components of the pump. The analysis is focused on the three coaxial parts that make out the cylinder, as these are subjected to the combined effect of pressure and thermal stresses. As shown in Figure 4, three parts are analyzed: the ring where the suction valve slides during its motion (A), the cylindrical part that constitutes the cylinder (B) and the seating for the piston seals (C). For the simulations it is assumed that components B and C are made from stainless steel AISI 630. Instead, part A is made from a copper-beryllium alloy C17200 TF00.

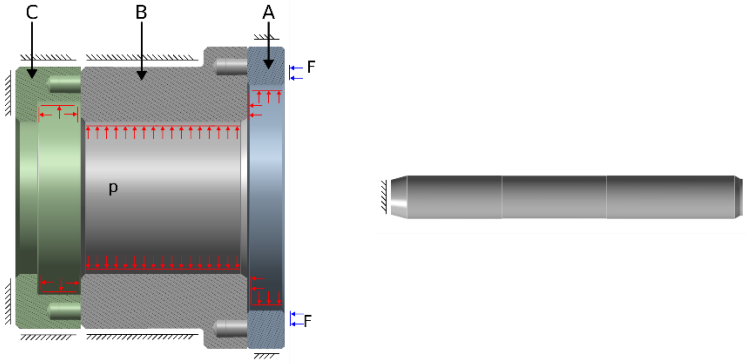

Figure 4. Sketch of components tested in structural simulations and boundary conditions. (a) Cylinder assembly: A, valve seat ring, B, cylinder body, C, piston ring seat. (b) Piston

The simulations are performed with the commercial software ANSYS Mechanical using a steady-state, three-dimensional approach. The solid domain is discretized into about $5 \cdot 10^5$ tetrahedral elements. The radial motion of the cylinder is controlled by imposing no radial deformation on the lateral surface of the three components. The axial motion of the assembly is prevented by introducing a rigid support on the bottom of the seat for the piston seals (C). On the top surface of component A, the compression force due to the assembly screws is imposed. A force of 10000 N acting on the inner half of the valve seat ring is calculated by assuming eight M8 screws at 70% of the yielding load.

Finally, the temperature distribution obtained from the thermal simulations is imposed (see Figure 2). The structural integrity and deformation of the three components are checked in the most critical conditions and using a conservative approach, by imposing the maximum pressure of 350 bar on all the internal surfaces of the cylinder. During the actual working cycle of the pump, the maximum pressure is reached only when the piston is found at the top dead center, hence the maximum pressure would be acting on a smaller surface.

In addition to simulating above-mentioned components, the radial deformation of the piston during pump operation is estimated, as the heat generated by friction may cause an expansion of the piston and the damaging of the pump. Hence, the temperature distribution calculated from

the thermal simulations is imposed, and a fixed support is assumed as boundary condition on the drivetrain side of the piston. (see Figure 4).

4. Results

In this Section the results from the CFD, thermal and structural simulations are shown. First, the distribution of the heat transfer coefficient obtained from the suction and discharge CFD simulations are shown in Sect. 4.1. Then, the results of the thermal simulations are shown in Sect. 4.2, followed by the results of the structural analysis in Sect. 4.3.

4.1. Heat transfer coefficient

The maps of the suction and discharge heat transfer coefficient obtained from the CFD simulations are shown in Figure 5. The value of the heat transfer coefficient can vary by an order of magnitude, depending on the fluid velocity. The minimum values are reached within the inner suction volume of the pump, where the fluid velocities are small. Instead, in the suction channels the fluid is accelerated due to the reduction in cross-sectional area and the heat transfer coefficient increases. In the discharge duct the maximum heat transfer coefficient is found in the throat area around the discharge valve, where the fluid velocity increases significantly.

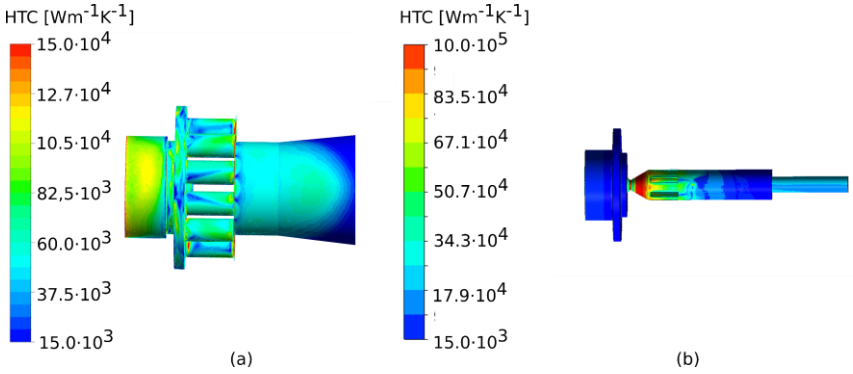

Figure 5. Distribution of heat transfer coefficient from the simulations of suction (a) and discharge (b) phases.

4.2. Thermal simulations

The resulting distribution of the heat transfer coefficient obtained from the CFD simulations is used as boundary condition in the thermal simulation. First, the most critical condition, corresponding to the maximum discharge pressure, is analyzed. The resulting temperature distribution is shown in Figure 6. The critical component is represented by the piston, which reaches temperature of up to 316K, about 240K larger than the liquid temperature. The piston heats up due to the friction between the piston and seals. In this pump configuration, the seals are fixed and most of the heat is absorbed by the piston. Instead, since only 10% of the frictional heat is transferred to the Teflon seals, and given their low conductivity, the cylinder is at an almost homogeneous temperature, with minimal differences from the liquid temperature.

In addition, the temperature distribution of the pump is affected by the heat transfer with the external ambience. Due to the vacuum chamber, where an adiabatic condition is imposed, the external surface of the pump around the vacuum chamber raises, as the pump is not cooled down by the liquid and is mainly affected by the natural convection. The external temperature of the pump is closer to the liquid temperature close to the suction and discharge fittings, where the heat transfer with the cryogenic liquid maintains a lower temperature. The warm end of the pump

is instead found at about 200 K due to the combined effect of the ambient heat transfer and conduction through the length of the pump.

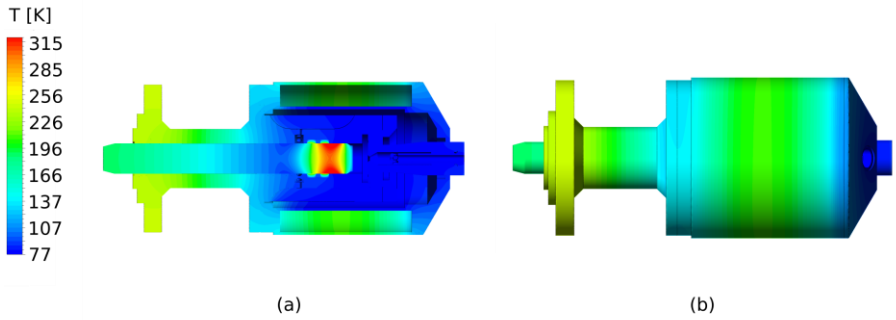

Figure 6. Steady temperature distribution obtained from the thermal simulations. (a) external temperature distribution. (b) Internal temperature distribution.

The thermal response of the pump is also evaluated for different discharge pressures at a constant rotational speed. Figure 7 shows a breakdown of the heat transfer contributions between the two heat sources, namely the friction heat and the heat transfer with the external ambience, and the heat exchange with the working fluid. In the latter case, the contributions of the suction and discharge lines, cylinder and piston are divided to provide further insight into the thermal response of the machine.

For the rotational speed and range of pressures analyzed, the most critical contribution is given by the friction between the piston and the cylinder. The additional thermal load caused by the increasing working pressures is absorbed completely by the fluid within the cylinder, where the liquid cools down the piston and seals during their relative motion. The critical component is represented by the piston, as differences in the working pressure can have a significant effect on its steady-state temperature distribution. Indeed, Figure 7 shows the temperature distribution for varying discharge pressure levels. Results show how increasing the maximum working pressure of the pump represents a complex challenge, as the temperature of the piston needs to be limited despite the increase in thermal load. In the analyzed configuration, the average temperature of the sliding surface of the piston shows an increase of 110 K when the pressure is raised from 150 to 350 bar.

4.3. Structural simulation

In the second part of this work, structural simulations of the pump under the combined influence of thermal and pressure loads are carried out. A simplified analysis is performed on the three components that constitute the cylinder (see Figure 4) as these are the most crucial in terms of loading. Figure 8 shows the distribution of the equivalent stresses calculated using Von Mises criterion, assuming a liquid pressure of 350 bar, equal to the maximum discharge pressure. The tested loading configuration is conservative with regard to the actual working conditions of the pump, as the maximum cycle pressure is applied in the simulations to all the cylinder surfaces (see Sect.3.3). In contrast, the pump is subjected to the maximum pressure only when the piston is located at the top dead center. Nevertheless, considering a yielding strength of 1000 MPa for the AISI 630 stainless steel and a yielding strength of 1170 MPa for the copper-beryllium alloy used in part A, the maximum stress is smaller than the yielding strength of the chosen materials. For the stainless steel AISI 630, the yielding stress at ambient temperature is used for comparison,

as no value is available in the literature at cryogenic temperatures. The maximum stresses are located on the cylindrical surface of component B (see Figure 4) due to the pressure of the fluid. The stress distribution is almost uniform on the cylindrical surface.

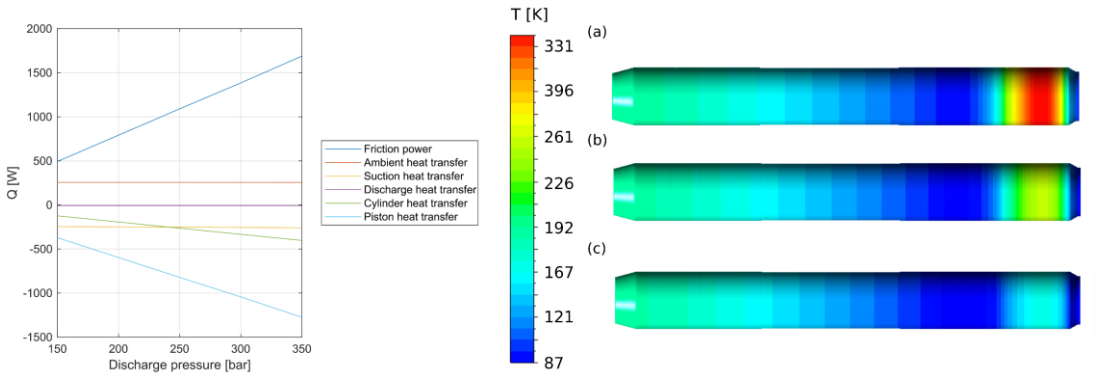

Figure 7. Temperature distribution of the piston: (a) 280 bar, (b) 180 bar, (c) 80 bar.

In addition to evaluating the stress distribution of the pump, the tolerances between piston and cylinder must be analyzed. Figure 9 (a) shows the radial deformation of the piston, under the combined action of the pressure and temperature gradients caused by the friction between piston and seals. Due to the cryogenic temperature the piston contracts in the radial direction by up to 43 μm. However, in the region that is heated up due to friction, the temperature is close to ambient value (see Figure 7), hence the diameter of the piston is close to the undeformed geometry.

The deformation distribution of the cylinder is shown in Figure 9 (b). For these components, the combined effect of pressure and temperature leads to minimal deformation from the undeformed geometry. Indeed, the pressure leads to an increase of the cylinder diameter while the cryogenic temperatures to a reduction. The final expansion is of the order of magnitude of 6 μm, hence the values are deemed acceptable for reliable running of the pump.

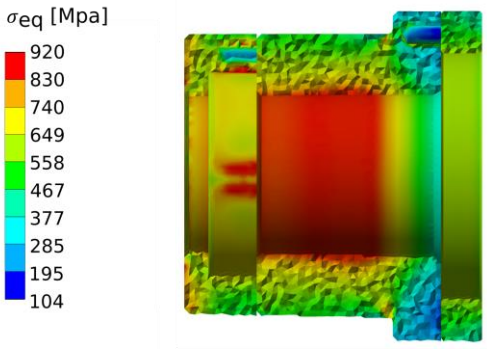

Figure 8. Equivalent stress distribution calculated with Von Mises criterion.

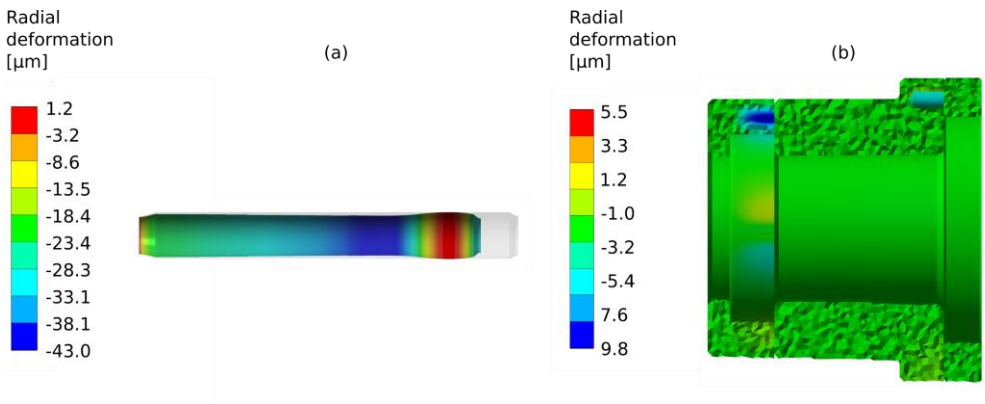

Figure 9. (a) Radial deformation distribution of the piston. The deformations are amplified by a factor of 62. The undeformed geometry of the piston is shown in grey. (b) radial deformation of the cylinder.

Conclusions

In this study, a simplified de-coupled methodology was presented to perform thermal and structural simulations of a cryogenic piston pump. This approach can aid the design process of these machines, providing further insight into the steady-state temperature distribution of the pump. In this way, the temperature distribution of piston and cylinder can be analysed, verifying that the effect of friction does not lead to excessive temperatures.

Additionally, simplified structural simulation can aid the verification of critical components and improvements can be identified at early stages of development reducing design times.

Results show that in the analysed prototype cryogenic pump, the piston represents the crucial component. Indeed, the power dissipated due to friction leads to piston temperatures up to 150K higher than the fluid temperature at the maximum pressure of 350 bar. Nevertheless, the temperature gradient does not induce excessive deformations of the piston, as it was shown from structural simulations.

In future work, experimental tests of the pump could be performed in order to compare the steady-state results obtained from the simulations and to verify the correct performance of the pump. Additionally, transient CFD simulations of the pump could be carried out to evaluate how unsteady phenomena may affect the temperature distribution of the components investigated in this work.

References

[1] Li J, Ramteke A, Youn E, Hansen E, Kratschmar K, Prakash A, Stager J and Ku A Y 2021 Liquid pump-enabled hydrogen refueling system for heavy duty fuel cell vehicles: Pump performance and J2601-compliant fills with precooling *International Journal of Hydrogen Energy* **46** 22018–29

[2] Biermann A E and Kohl R C 1959 *Preliminary Study of a Piston Pump for Cryogenic Fluids*

[3] Lue J W, Miller J R, Walstrom P L and Herz W 1981 *Test of a cryogenic helium pump* (Oak Ridge National Lab., TN (USA))

[4] Yamane K, Nakamura S, Nosset T and Furuhama S 1996 A study on a liquid hydrogen pump with a self-clearance-adjustment structure *International Journal of Hydrogen Energy* **21** 717–23

[5] Cioni S, Balduzzi F, Romani L, Bianchini A and Ferrara G 2022 Fluid dynamic analysis of a cryogenic piston pump *J. Phys.: Conf. Ser.* **2385** 012037